



## Investigating the effect of deposition time on the morphology, structure and optical band gap of PbS thin films synthesized by CBD technique

Fekadu Gashaw Hone, Francis Kofi Ampong, Tizazu Abza, Isaac Nkrumah, Robert Kwame Nkum and Francis Boakye  
Kwame Nkrumah University of Science and Technology, Department of Physics, Ghana.

### ARTICLE INFO

#### Article history:

Received: 17 September 2014;

Received in revised form:

27 October 2014;

Accepted: 10 November 2014;

#### Keywords

Lead sulphide thin film,  
Nanocrystalline,  
Chemical bath deposition,  
Preferred orientations.

### ABSTRACT

Nanocrystalline lead sulphide thin films have been deposited on glass substrates from chemical baths containing lead acetate, sodium hydroxide, ammonia and thiourea at a bath temperature of 90 °C and a pH of about 12. Three different samples were prepared with deposition times of 30, 45 and 60 minutes respectively. The films were characterized using a variety of techniques. X-ray diffraction analyses revealed that all the films were polycrystalline in nature with the diffraction peaks indexed to the face centered cubic structure. The deposition time strongly influenced the preferred orientations of the crystallites as well as structural parameters such as average crystallite size, strain and dislocation density. SEM micrographs of all the films showed a highly compact surface composed of sharp-edged cubic shaped grains of different sizes. The elemental compositions of the films were confirmed by energy dispersive X-ray spectroscopy. The optical band gap of the films decreased from 1.32 eV to 1.10 eV with increasing deposition time.

© 2014 Elixir All rights reserved.

### Introduction

Lead sulphide (PbS) is the most studied material, among the group IV–VI compound semiconductors because of its potential applications in nonlinear optical devices [1]. Due to its functional nature, it has been widely used in many fields such as Pb<sup>2+</sup> ion exchange sensor, photography and as a solar absorber [2]. Its emission and absorption lines are consequently broader, but by varying its crystallite size, tunable emissions can be obtained within a large spectral region, ranging from the visible to near infrared. This spectral range is of great interest for fabricating light sources (including lasers) or optical amplifiers [3]. Quantum-sized PbS can be useful in many applications, particularly in electroluminescent devices such as light emitting diodes and high speed switching and IR detectors. These films are still widely used because of their good performance and cheap fabrication method, as well as their operation in the 0.7 – 3 μm range. In solar energy research, PbS thin films have been investigated for photothermal conversion applications, either independently, on metallic substrates or in multilayer stacks of PbS-CdS-PbS, (PbS)<sub>1-x</sub>(CdS)<sub>x</sub> composites [4]. PbS has been also recommended as an earth abundant sustainable material for affordable photovoltaic devices [5]. PbS has a face centered cubic crystal structure with space group  $Fm\bar{3}m$  and a narrow direct band gap of 0.41 eV at room temperature and an optical absorption coefficient of  $>10^5 \text{ cm}^{-1}$  [6-8]. PbS exhibits strong quantum size effects below excitonic Bohr radius of 18 nm and hence the energy band gap of its nanocrystals can be tuned to anywhere between 0.41 eV (bulk) to 4 eV. This makes the quantum confinement effect important in these films [9], both p-type and n-type PbS compounds can be made by doping [8, 10].

A wide variety of techniques are available for the deposition of PbS thin films such as; Successive ionic layer adsorption and reaction [11], Spray pyrolysis [12], Thermal evaporation method, [13], Electro-deposition [14], Photoaccelerated

chemical deposition [15] and Chemical bath deposition (CBD) [16, 17].

Among these techniques, metal chalcogenide thin films preparation by chemical deposition methods are currently attracting considerable attention as it is relatively inexpensive, simple and convenient for large area deposition. A variety of substrates such as insulators, semiconductors or metals can be used since these are low temperature processes which avoid oxidation and corrosion of substrate [18]. Additional advantages the CBD has over other techniques are; reproducibility, nonhazardous and well suitable for large area deposition at relatively low temperatures [19] (Bhushan, Mukherjee et al. 2002). The characteristics of chemical bath deposited thin films depend strongly on the growth condition by changing the deposition key parameters like bath temperature, deposition time, concentration of reactants, bath pH etc, one can control thickness, size of the nanoparticles and the energy band gap of the obtained thin films [20, 21]. In this paper, we report on the effect of deposition time on the morphology, structure and optical band gap of nanocrystalline PbS thin films deposited by CBD technique.

### Materials and Methods

#### Substrate Preparation

Commercially available glass slides with a size of 75 mm × 25 mm × 2 mm were used as substrates for the deposition of PbS thin films. The microscope glass slides were degreased in nitric acid over night and subsequently kept in ethanol for about 30 minutes, then ultrasonically cleaned with distilled water and dried under ambient conditions before being used for the deposition.

#### Deposition of the thin film

The chemicals used were lead acetate dehydrate, (Pb(CH<sub>3</sub>COO)<sub>2</sub>•3H<sub>2</sub>O), as the source of lead ions and thiourea (CS(NH<sub>2</sub>)<sub>3</sub>) which provided sulphur ions. Sodium hydroxide, (NaOH) and Ammonia (NH<sub>3</sub>) were used as a complexing agent and to also maintain the alkalinity of the chemical bath. All the

chemicals used were of analytical grade. The mixture for the bath was prepared by mixing an appropriate amount of lead acetate and 10 ml of NaOH in a 100 ml beaker. Initially, the solution looked milky turbid due to the formation of  $\text{Pb}(\text{OH})_2$  it later changed into a colorless solution after the addition of a sufficient amount of  $\text{NH}_3$ . 5 ml of thiourea and some distilled water was then added to obtain a final volume of 70 ml. The cleaned substrates were immersed vertically into the solution with the help of a substrate holder. The reaction mixture was continuously stirred with a magnetic stirrer and maintained at a temperature of  $90^\circ\text{C}$  for deposition. The prepared solution was initially clear and colorless but turned to yellowish after a few minutes and later, a mirror-like film began to deposit onto the sides of the beaker and the substrate confirming the formation of PbS. Three different samples were prepared with deposition times of 30, 45 and 60 minutes respectively. After deposition, the samples were removed from the solution, rinsed ultrasonically with distilled water and dried under ambient conditions before film characterization. All deposited PbS thin films were mirror-like with a grey color, homogeneous, well adherent, and specularly reflecting.

#### Characterization of the thin film

The crystallographic structure of PbS thin films were analyzed with a PANalytical Empyrean Series 2 powder X-ray diffractometer with a  $\text{Cu-K}\alpha$  radiation ( $\lambda_{\alpha 1} = 1.5406 \text{ \AA}$  and  $\lambda_{\alpha 2} = 1.5443 \text{ \AA}$ ) source over the diffraction angle  $2\theta$  between  $5^\circ$  and  $80^\circ$ . The machine was operated at 40 mA and 45 KV. The elemental composition and surface morphology of the samples were determined using energy dispersive X-ray analysis (EDX) attached to a Zeiss 1550 VP scanning electron microscope (SEM) operating with an accelerating voltage 20 kV. Optical absorption spectra were measured at room temperature, using a Shimadzu UV/Vis mini-1240 Spectrophotometer within the wavelength range of 200 nm – 1100 nm.

#### Results and Discussion

##### X-ray diffraction analysis

The X-ray diffraction patterns of the as-deposited PbS thin films for the different deposition times are shown in Figures 1a, 1b and 1c. The well defined peaks observed in all three samples correspond to reflections from the (111), (200), (220), (311), (222), (400), (331), (420) and (422) planes of the face centered cubic structure (Galena, JCPDS file number 005-0592).

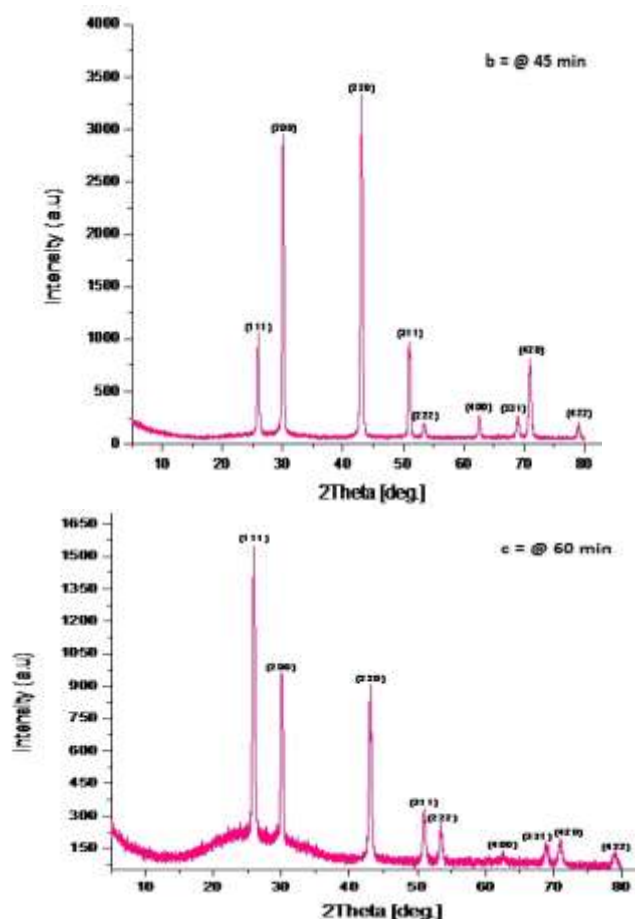
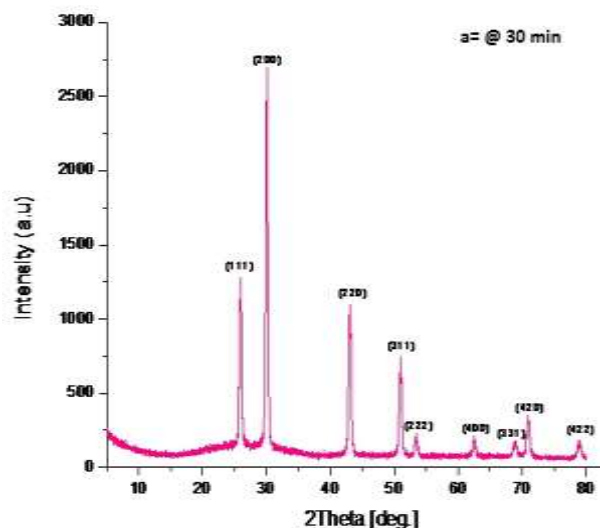


Fig 1. XRD patterns of PbS thin films prepared at different deposition time

The sharpness of the peaks in the X-ray diffraction pattern reveals the good crystallinity of the films and also confirms the stoichiometric nature of the PbS films (Deshpande et. al., 2013). No impurity peaks such as  $\text{PbO}$ ,  $\text{PbS}_2$  are observed, indicating that the as-deposited PbS nanocrystallines thin films are of high purity. From the XRD patterns it can be observed that the preferred orientations of the crystallites vary with deposition time. For a deposition time of 30 minutes the crystallites had a preferred orientation along the (200) plane, whilst for the deposition time of 45 and 60 minutes, the crystallites had a preferred orientation along the (220) and (111) planes respectively, suggesting a three dimensional growth of the as-deposited thin films [11]. Similar observations were reported by [22, 23]. Lattice constant ( $a_{hkl}$ ) for the cubic structure was calculated using Eq. (1) and the results are presented in Table 1.

$$a_{hkl} = d_{hkl} \sqrt{h^2 + k^2 + l^2} \quad (1)$$

The calculated value of the lattice constant ' $a_{hkl}$ ' of the films show a slight deviation from its standard value of  $5.9362 \text{ \AA}$ . Corrected values for the lattice constants are estimated from the Nelson-Riley (N-R) plots, derived from the equation [24].

$$f(\theta) = \frac{1}{2} \left( \frac{\cos^2 \theta}{\sin \theta} + \frac{\cos^2 \theta}{\theta} \right) \quad (2)$$

where  $\theta$  is the Bragg angle and  $f(\theta)$  is an error function. The N-R plot is obtained by plotting the calculated ' $a_{hkl}$ ' for each plane against the corresponding error function. The intersection at  $f(\theta) = 0$  gives the corrected value of the lattice parameter which is more or less free from systematic errors [25]. Fig.2 shows a typical N-R plot of lattice parameter  $a(\text{\AA})$  versus the

error function  $f(\theta)$  for the PbS thin film deposited at 30 minutes. Similar graphs were obtained for the films with deposition time of 45 and 60 minutes. The values are presented in Table 1.

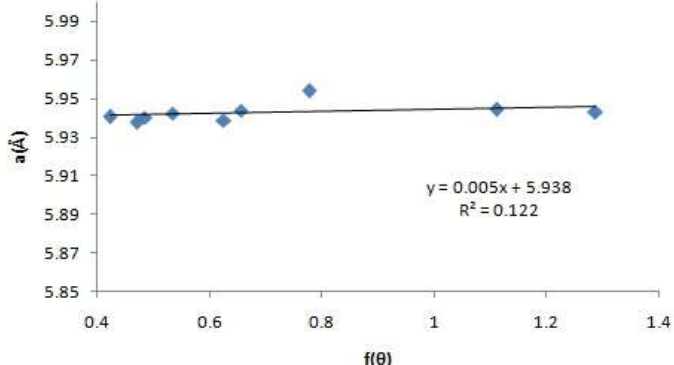


Fig 2. Nelson–Riley plot for a PbS thin film deposited at 30 min

All the parameters obtained from the XRD data for the as-deposited PbS thin films are compared with standard data and presented in Table 1.

The texture coefficient (TC) represents the texture of the particular plane, deviation of which from unity implies the preferred growth. Quantitative information concerning the preferential crystallite orientation was obtained from the texture coefficient  $TC(hkl)$  defined as [26].

$$TC(hkl) = \frac{I(hkl)}{\sum_n I_o(hkl)} \times 100\% \tag{3}$$

Where  $I(hkl)$  is the measured relative intensity of a plane ( $hkl$ ),  $I_o(hkl)$  is the standard intensity of the plane ( $hkl$ ) taken from the JCPDS data,  $n$  is the number of diffraction peaks. The value  $TC(hkl) = 1$  represents films with randomly oriented crystallites, while higher values indicate the abundance of grains oriented in a given ( $hkl$ ) direction [22, 26]. The calculated texture coefficients are presented in table 1. The results indicate that: for a deposition time of 30 minutes, the crystallites are oriented in the (200) plane and for a deposition time of 45 minutes, the crystallites are oriented in the (220) plane, and (111) plane for a deposition time of 60 minutes.

The average crystallite size ( $D$ ) was calculated from the X-ray diffraction pattern, using the Scherrer (1918), formula which is given as:

$$D = \frac{K \lambda}{\beta_{2\theta} \cos\theta} \tag{4}$$

where,  $\theta$  is the diffraction angle,  $\beta$  is the full width at half maximum of the most intense peak measured in radians,  $K$  is the constant known as the shape factor, taken as 0.94 [7] and  $\lambda$  is the wave length of the X-ray radiation. The average crystallite size of the films increased linearly with deposition time from 20 nm for a deposition time of 30 minutes, to 32 nm for a deposition time of 60 minutes. Figure 3 shows the variation of crystallite size with deposition time.

The deviation of the calculated lattice constant from the bulk sample value mentioned earlier, shows that the crystallites may be under some strain or/and the presence of residuals of the reaction components in the films [1, 3]. The microstrain value ( $\epsilon$ ) of the as-deposited PbS thin films were evaluated by using the following mathematical relation [23, 27]:

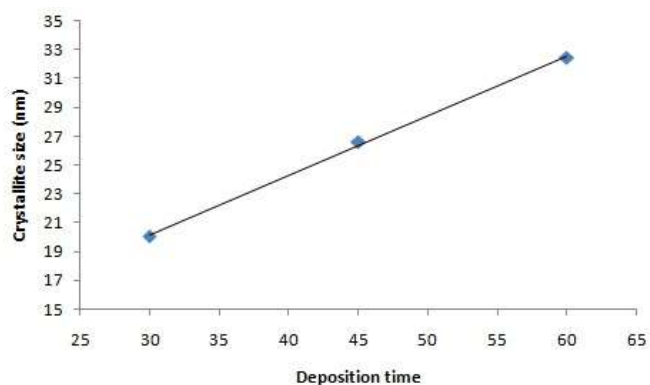


Fig. 3 Variation of crystallite size with deposition time

$$\epsilon = \frac{\beta \cos\theta}{4} \tag{5}$$

Where  $\theta$  and  $\beta$  are as defined in equation 2. The other structural parameter calculated is the dislocation density ( $\delta$ ) which is a measure of the defects in the film [28], and this was calculated by using Williamson and Smallman’s formula [29]:

$$\delta = \frac{n}{D^2} \tag{6}$$

Where  $n$  is a factor, which equals unity for a minimum dislocation density and  $D$  is the crystalline size [30, 31]. Strain and dislocation density were calculated from the most intense peak of the X-ray diffraction pattern for each PbS thin films deposited at different deposition time. The results are tabulated in Table 2.

From table 2, it can be observed that the dislocation density and strain decreases with increasing deposition time. Since dislocation density and strain are the manifestation of dislocation network in the films, the decrease in dislocation density indicates the formation of high quality films [27]. As the dislocation density is the measure of the defects in the crystalline structure, the smaller value of  $\delta$  obtained for the film deposited at 60 minutes, suggests the film has a comparatively higher degree of crystallinity.

**Elemental analysis and morphological studies**

The SEM micrographs of the as-deposited PbS thin films taken at a magnification of x 60 K and EDX analysis are shown in Figures 4a, 4b and 4c. The EDX analysis for all the three samples revealed that the atomic percentage of Pb:S is very close to 1 indicating that the thin films have the desired stoichiometric ratio. No significant change was observed on Pb:S atomic ratio due to the variation of deposition time.

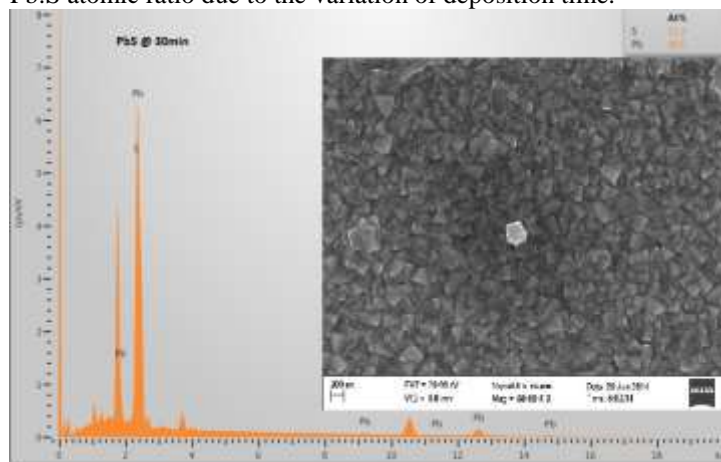


Fig 4a. EDX spectra and SEM micrograph of PbS thin film deposited at 30 min

Table 1. Crystallographic parameters of PbS thin films obtained from XRD analysis

Deposition time	2θ in degree	d-space in Å			Cell parameter in Å		Corrected cell parameter in Å	Crystalline size (D)(nm)	TC%
		hkl Planes	standard	Observed	standard	calculated			
30 min	25.970	111	3.4290	3.4310		5.9426		10.54	
	30.067	200	2.9690	2.9721		5.9442		20.08	
	42.968	220	2.0990	2.1050		5.9538		12.32	
	50.954	311	1.7900	1.7922	5.9362	5.9440		14.11	
	53.445	222	1.7140	1.7144		5.9388	5.938	6.56	
	62.522	400	1.4840	1.4856		5.9424		9.54	
	68.904	331	1.3620	1.3628		5.9403		6.76	
	70.992	420	1.3270	1.3277		5.9376		11.93	
45 min	78.952	422	1.2120	1.2126		5.9405		8.35	
	26.012	111	3.4290	3.4255		5.9331		5.59	
	30.046	200	2.9690	2.9742		5.9484		14.34	
	43.065	220	2.0990	2.0987		5.9360		26.59	
	51.065	311	1.7900	1.7871		5.9271		12.83	
	53.549	222	1.7140	1.7099	5.9362	5.9233	5.921	3.62	
	62.575	400	1.4840	1.4832		5.9328		9.05	
	69.017	331	1.3620	1.3597		5.9268		8.72	
60 min	71.041	420	1.3270	1.3258		5.9291		10.85	
	79.054	422	1.2120	1.2103		5.9292		6.25	
	25.968	111	3.4290	3.4312		5.9430		32.47	
	30.154	200	2.9690	2.9638		5.9276		9.86	
	43.088	220	2.0990	2.0994		5.9381		19.17	
	51.033	311	1.7900	1.7896	5.9362	5.9354		8.24	
	53.529	222	1.7140	1.7119		5.9302	5.932	10.93	
	62.599	400	1.4840	1.4839		5.9356		4.46	
68.966	331	1.3620	1.3617		5.9355		10.57		
71.005	420	1.3270	1.3275		5.9368		7.88		
79.072	422	1.2120	1.2111		5.9331		7.35		

Table 2. Calculated microstructural parameters and optical band gap energy

Deposition time	2θ in degree	hkl Planes	FWHM (β) in 2θ	Energy band gap (eV)	Strain ε lines <sup>2</sup> m <sup>-4</sup>	Dislocation density (δ) lines/m <sup>2</sup>
30 min	30.067	200	0.4133	1.32	1.742x10 <sup>-3</sup>	2.48x10 <sup>15</sup>
45 min	43.065	220	0.3120	1.22	1.266 x10 <sup>-3</sup>	1.41x10 <sup>15</sup>
60 min	25.968	111	0.2558	1.10	1.088 x10 <sup>-3</sup>	0.95x10 <sup>15</sup>

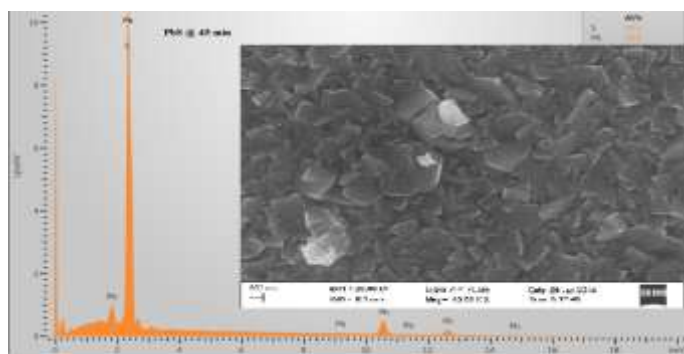


Fig 4b. EDX spectra and SEM micrograph of PbS thin film deposited at 45 min

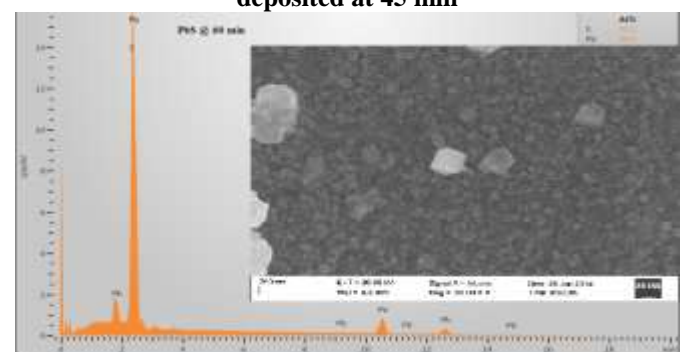


Fig 4c. EDX spectra and SEM micrograph of PbS thin film deposited 60 min

The SEM micrographs show the surface morphology is composed largely of compact sharp edged cubic shaped grains, of different sizes and uniformly distributed over a smooth homogenous background without visible defects such as, cracks, peeling or pinholes. The micrograph of the film deposited at 45 minutes shows a plate-like morphology. Similar morphology has been reported by [32]. From the SEM micrographs it is easily observed that the deposition time plays a vital role on the morphological properties of the nanocrystalline PbS thin films.

#### Determination of the Optical Band gap

The energy band gap and transition type were determined from mathematical treatment of data obtained from optical absorbance versus wavelength, with the Stern (1963), relationship of near-edge absorption which is given as [33].

$$A = \frac{[K(h\nu - E_g)]^{n/2}}{h\nu} \quad (7)$$

where  $\nu$  is the frequency,  $h$  is the Planck's constant,  $k$  is a constant while  $n$  carries the value of either 1 for direct transition or 4 for indirect transition. PbS is a direct band gap material [34], thus  $n$  is taken as 1. The energy band gap is obtained by extrapolating the linear portion of  $(Ah\nu)^2$  versus  $h\nu$  to the energy axis at  $(Ah\nu)^2 = 0$ . The linear nature of the plot of  $(Ah\nu)^2$  versus  $h\nu$  shown in Fig.5 verifies the presence of a direct transition [35]. From the plot it was observed that the band gap decreased from 1.32 eV to 1.10 eV as the deposition time increased from

30 minutes to 60 minutes. Similar observations have been reported by [22, 23].

The variation of energy gap for all the as-deposited PbS thin films are summarized in table 2. The estimated band gap is slightly higher when compared to the reported bulk value of 0.41 eV, this may be attributed to quantum size effects induced by the nanocrystallites in the PbS thin film [10, 23].

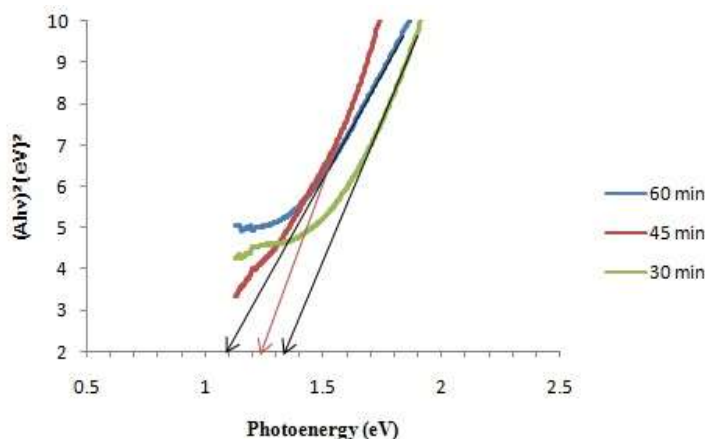


**Fig 5. A graph of  $(Ah\nu)^2$  plotted as a function of the photon energy ( $h\nu$ ) for PbS thin film for different deposition time.**

#### Conclusion

Well adherent PbS thin films were synthesized by CBD technique and the effect of deposition time on their structural, morphological and optical band gap, investigated. X-ray diffraction studies revealed that the thin films had a cubic rock salt structure with good crystallinity. The dependence of the preferred orientation of the crystallites as well as other structural parameters such as strain and dislocation on the deposition time has been well established. From the SEM micrographs, the surface morphology of the thin films is composed largely of cubic shaped grains, uniformly distributed over a smooth homogenous background. However, the film deposited at 45 minutes showed a plate-like structure. The EDX analysis for all PbS samples revealed that the atomic percentage of Pb:S is very close to 1. The optical band gap of the films decreased from 1.32 eV to 1.10 eV with increasing deposition time. The larger optical band gap of the thin films compared with the bulk value can be attributed to quantum size effects.

#### Acknowledgement:

One of the authors Fekadu Gashaw Hone would like to acknowledge Intra-ACP academic mobility scheme for financial support for the research work.

#### References:

[1] N. Choudhury, B.K. Sarma, Structural analysis of chemically deposited nanocrystalline PbS films, *Thin Solid Films*, 519 (2011) 2132-2134.  
 [2] S.B. Qadria, A. Singhb, M. Yousuf, Structural stability of PbS films as a function of temperature, *Thin Solid Films*, 431/432 (2003) 506-510.  
 [3] C.Rajashree, A.R. Balu, V.S.Nagarethinam, Substrate Temperature effect on the Physical properties of Spray deposited Lead sulfide Thin Films suitable for Solar control coatings, *Int.J. ChemTech Res.*, 6 (2014) 347-360.  
 [4] L.P. Deshmukh, B.M. More, S.G. Holikatti, P.P. Hankare, Preparation and properties of  $(\text{CdS})_x - (\text{PbS})_{1-x}$  thin-film composites, *Bulletin of Materials Science*, 17 (1994) 455-463.  
 [5] W. Cyrus, A.P. Alivisatos, D.M. Kammen, Materials availability expands the opportunity for large-scale

photovoltaics deployment, *Environ. Sci. Technol.*, 43 (2009) 2072-2077.

[6] M. Karabulut, H. Ertap, H. Mammadov, G. Ugurlu, M.K. Ozturk, Properties of PbS thin films grown on glass and layered GaSe crystal substrates by chemical bath deposition, *Turkish Journal of Physics*, 38 (2014) 104-110.

[7] N. Choudhury, B.K. Sarma, Structural characterization of lead sulfide thin films by means of X-ray line profile analysis, *Bull. Mater. Sci.*, 32 (2009).

[8] S.I. Sadovnikov, A.I. Gusev, Structure and properties of PbS films, *Journal of Alloys and Compounds*, 573 (2013) 65-75.

[9] O.P. Moreno, M.C. Portillo, M.M. Flores, J.M. Juárez, G.A. Ávila, R.L. Morales, O.Z. Ángel, Properties of Chemical Bath Deposited PbS Thin Films Doped with  $\text{Cd}^{2+}$ , *Journal of Materials Science and Engineering A*, 1 (2011) 759-767.

[10] N.B. Kotadiya, A.J. Kothari, D. Tiwari, T.K. Chaudhuri, Photoconducting nanocrystalline lead sulphide thin films obtained by chemical bath deposition, *Appl. Phys. A*, 108 (2012) 819-824.

[11] K.C. Preetha, K.V. Murali, A.J. Ragina, K. Deepa, T.L. Remadevi, Effect of cationic precursor pH on optical and transport properties of SILAR deposited nano crystalline PbS thin films, *Current Applied Physics*, 12 (2012) 53-59.

[12] R. Thiagarajan, M.M. Beevi, M. Anusuya, T. Ramesh, Influence of reactant concentration on nano crystalline PbS thin films prepared by Chemical Spray Pyrolysis, *Optoele. and Adv. Matte.*, 6 (2012) 132-135.

[13] A.J. Mohammed, S.R. Salim, M.S. Jaleel, M.A.M. Hassan, Structural Characterization of Lead Sulfide Thin Films by Means of FTIR Analysis after Irradiation of B-ray, *British Journal of Science*, 7 (2012) 33-35.

[14] Y. Gülen, M. Alanyahoğlu, K. Ejderha, Ç. Nuhuğlu, A. Turut, Electrical and optical characteristics of Au/PbS/n-6H-SiC structures prepared by electrodeposition of PbS thin film on n-type 6H-SiC substrate, *Journal of Alloys and Compounds*, (2011) 3155-3159.

[15] P.K. Nair, V.M. Garcia, A.B. Hernandez, M.T.S. Nair, *J.Phys.D: Appl.Phys.*, 24 (1991) 1466-1472.

[16] S. Seghaier, N. Kamoun, R. Brini, A.B. Amara, Structural and optical properties of PbS thin films deposited by chemical bath deposition, *Materials Chemistry and Physics*, 97 (2006) 71-80.

[17] F.Göde, E.Güneri, F.M.Emen, V.EmirKafadar, S.Ünlü, Synthesis, structural, optical, electrical and thermoluminescence properties of chemically deposited PbS thin films, *Journal of Luminescence*, 147 (2014) 41-48.

[18] R.S. Mane, C.D. Lokhande, Chemical deposition method for metal chalcogenide thin films, *Materials Chemistry and Physics*, 65 (2000) 1-31.

[19] S.A. Pawar, R.S. Devan, D.S. Patil, A.V. Moholkar, M.G. Gang, Y.-R. Ma, J.H. Kim, P.S. Patil, Improved solar cell performance of chemosynthesized cadmium selenide pebbles, *Electrochimica Acta*, 98 (2013) 244-254.

[20] N. Ghobadi, R. Moradian, Strong localization of the charge carriers in CdSe nanostructural films, *International Nano Letters*, 3 (2013) 1-5.

[21] A. Hussain, A. Begum, A. Rahman, Electrical and optical properties of nanocrystalline lead sulphide thin films prepared by chemical bath deposition, *Indian J Phys*, 86 (2012) 697-701.

[22] A.S. Obaid, M.A. Mahdi, A.A. Dihe, Z. Hassan, Effect of Deposition Time on the PbS Thin films Prepared using Microwave-Assisted Chemical Bath Deposition: Structure and Optical Characterization, *International Conference on Education, Applied Sciences and Management*, (2012) 1-4.

- [23] T. Tohidi, K. Jamshidi-Ghaleh, A. Namdar, R. Abdi-Ghaleh, Comparative studies on the structural, morphological, optical and electrical properties of nanocrystalline PbS thin films grown by chemical bath deposition using two different bath compositions, *Materials Science in Semiconductor Processing*, (2013).
- [24] A.U. Ubale, A.R. Junghare, N.A. Wadibhasme, A.S. Daryapurkar, R.B. Mankar, V.S. Sangawar, Thickness Dependent Structural, Electrical and Optical Properties of Chemically Deposited Nanoparticle PbS Thin Films, *Turk J. Phys.*, 31 (2007) 279-286.
- [25] M.P. Deshpande, N. Garg, S.V. Bhatt, P. Sakariya, S.H. Chaki, Characterization of CdSe thin films deposited by chemical bath solutions containing triethanolamine, *Materials Science in Semiconductor Processing*, 16 (2013) 915-922.
- [26] S. Ilican, M. Caglar, Y. Caglar, Determination of the thickness and optical constants of transparent indium-doped ZnO thin films by the envelope method, *Materials Science-Poland*, 25 (2007) 709-718.
- [27] M.R.A. Bhuiyan, M.A.A. Azad, S.M.F. Hasan, Annealing effect on structural and electrical properties of AgGaSe<sub>2</sub> thin films *Indian Journal of pure and Applied Physics*, 49 (2011) 180-185.
- [28] G.K. Williamson, R.E. Smallman, Dislocation Densities in Some Annealed and Cold-Worked Metals from Measurements on the X-Ray Debye-Scherrer Spectrum, *Philosophical Magazine*, 1 (1956) 34-45.
- [29] K. Sarmah, R. Sarma, H.L. Das, Structural Characterization of Thermally Evaporated CdSe thin films, *Chalcogenide Letters*, 5 (2008) 153-163.
- [30] K.S. S. Thanikaikarasana, T. Mahalingam, S. Velumani and Jin-Koo Rhee, Electrodeposition and characterization of Fe doped CdSe thin films from aqueous solution, *Materials Science and Engineering B*, 174 (2010) 242-248.
- [31] B. Altokka, M.C. Baykul, M.R. Altokka, Some physical effects of reaction rate on PbS thin films obtained by chemical bath deposition, *Journal of Crystal Growth*, 384 (2013) 50-54.
- [32] K. Anuar, W.T. Tan, M. Jelas, S.M. Ho, S.Y. Gwee, Effects of Deposition Period on the Properties of FeS<sub>2</sub> Thin Films by Chemical Bath Deposition Method, *Thammasat Int. J. Sc. Tech.*, 15 (2010) 62-69.
- [33] S. Thangavel, S. Ganesan, K. Saravanan, Annealing effect on cadmium in situ doping of chemical bath deposited PbS thin films, *Thin Solid Films*, 520 (2012) 5206-5210.
- [34] C.D. Lokhande, R.B. Kale, Band gap shift, structural characterization and phase transformation of CdSe thin films from nanocrystalline cubic to nanorod hexagonal on air annealing, *Semiconductor Science and Technology* 20 (2005) 1-9.